

## $^{18}\text{F}$ -FDG PET/CT compared with ultrasound and biopsy for detection of vasculitis of the temporal artery branches

Rottenburger Christof<sup>a\*</sup>, Mensch Noemi<sup>b\*</sup>, Imfeld Stephan<sup>c</sup>, Aschwanden Markus<sup>c</sup>, Glatz Katharina<sup>d</sup>, Staub Daniel<sup>c</sup>, Berger Christoph T.<sup>ef</sup>, Daikeler Thomas<sup>b</sup>

<sup>a</sup> Division of Nuclear Medicine, University Hospital Basel, Switzerland

<sup>b</sup> Department of Rheumatology, University Hospital Basel, Switzerland

<sup>c</sup> Department of Angiology, University Hospital Basel, Switzerland

<sup>d</sup> Pathology, Institute of Medical Genetics and Pathology, University Hospital Basel, University of Basel, Switzerland

<sup>e</sup> Department of Internal Medicine, University Hospital Basel, Switzerland

<sup>f</sup> Department of Biomedicine, Translational Immunology, University of Basel, Switzerland

### Summary

**AIMS:** To describe the feasibility and diagnostic accuracy of  $^{18}\text{F}$ -FDG positron emission tomography-computed tomography (PET/CT) of the temporal artery compared with temporal artery ultrasound and histology of the temporal artery in patients with suspicion of having giant cell arteritis (GCA).

**MATERIALS AND METHODS:** Patients with suspected GCA were included. PET/CT standard uptake value ratios and the compression sign on ultrasound were assessed for the trunk, and parietal and frontal branches of the temporal artery. Temporal artery biopsies were systematically re-assessed, if available.

**RESULTS:** In 17/34 patients, GCA was confirmed. Temporal artery PET/CT confirmed vasculitis in 9/17 patients and was negative in all 17 controls. Nineteen of 34 subjects had a temporal artery biopsy, which was positive in 7 patients. Five of these seven were negative in the preceding PET/CT. Ultrasound confirmed vasculitis in 9/17 patients and was negative in 16/17 controls. In 7/17 patients, PET/CT and ultrasound were positive for temporal arteritis. Two patients had positive findings only on temporal artery PET/CT and two patients showed vasculitis only on temporal artery ultrasound. No temporal artery segments <1.4 mm were positive on PET/CT. The parietal branches were PET/CT-positive in two patients only. In contrast, on ultrasound vasculitic findings were equally distributed amongst all branches. Sensitivity and specificity for identification of temporal artery involvement was 53% and 100% for PET/CT, and 53% and 94% for ultrasound, respectively.

**CONCLUSIONS:** Assessment of the temporal artery with PET/CT is a valuable extension in the diagnostic workup for GCA. PET/CT and ultrasound have comparable diagnostic accuracy, but differ on a segment and a patient level and may thus be used as complementary tests. PET/

CT has a lower sensitivity for the parietal branch than ultrasound and histology.

### Introduction

$^{18}\text{F}$ -fluorodeoxyglucose ( $^{18}\text{F}$ -FDG) positron emission tomography-computed tomography (PET/CT) has been validated for the diagnosis of large-vessel vasculitis in several studies [1, 2]. The recent European League Against Rheumatism (EULAR) guidelines on diagnosis of giant cell arteritis (GCA) recommended PET/CT as one of the preferred imaging methods to assess large-vessel vasculitis [3]. Recently, specific PET/CT protocols, facilitating evaluation of the temporal arteries, have been reported. Applying these protocols and using advanced PET/CT scanners with higher resolution properties allows the detection of increased  $^{18}\text{F}$ -FDG uptake of the temporal arteries in GCA [4].

A Danish study included 44 patients who were corticosteroid-naïve at the time of the PET/CT scan. Inflammation of the temporal and maxillary arteries was assessed visually [5]. Sensitivity and specificity of PET/CT for diagnosis of cranial GCA were 64% and 100%, respectively. Another cross-sectional study reported a sensitivity of 71% and specificity of 91% for whole body PET/CT, including a temporal artery protocol [6]. These studies used the 1990 American College of rheumatology (ACR) GCA classification criteria [7] as the reference for GCA diagnosis. Similar results for the diagnostic accuracy were obtained in a Dutch study, revealing a sensitivity and specificity of 79% and 92% in temporal artery biopsy-positive GCA patients [8].

Although these studies established the first evidence for the diagnostic usefulness of PET/CT in cranial GCA, they included only patients with symptoms and findings of cranial arteritis. Moreover, vasculitis was defined by visual grading without reporting of detailed segmental distribution [5, 6]. Semiquantitative assessment with measurement

\* Contributed equally to this work.

**Correspondence:**  
Prof. Thomas Daikeler,  
MD, Department of  
Rheumatology, University  
Hospital Basel, Peters-  
graben 4, CH-4031 Basel,  
Thomas.daikeler[at]usb.ch

of the standard uptake value (SUV) was performed in the Dutch study [7]. However, direct comparison of individual temporal artery segments' SUV to ultrasound and histology has not been reported up to now. The measurement of SUV provides several advantages, including the potential for disease monitoring in serial measurements and higher reader independency.

Here, we evaluated all three temporal artery segments with PET/CT in direct comparison with ultrasound and histology, using an adapted PET/CT acquisition protocol to enable optimisation of temporal artery PET/CT imaging without additional burden to the patient. The aim of this study was a direct comparison of temporal artery PET/CT findings with ultrasound and/or biopsy on a branch and on a patient level.

## Material and methods

### Ethics approval

The local ethics committee approved the study (Ethikkommission Nordwest- und Zentralschweiz, Number/ID of the approval 239/09).

### Patient cohort

Participating patients were recruited from our ethics committee-approved prospective cohort of patients with suspected GCA at the University Hospital Basel, Switzerland, for which all subjects provided written informed consent. We included in the analysis all consecutive patients who underwent PET/CT and ultrasound at our institution between August 2015 and January 2019 with the indication of suspected GCA. Clinical parameters and laboratory results were retrieved from our local cohort database and from the electronic patient records. Ultrasound images of the temporal arteries, as well as histological slides from temporal artery biopsies, were systematically reassessed. The final diagnosis of GCA was made according to published criteria used in interventional studies [9, 10].

### PET/CT protocol for assessing the temporal artery

All patients underwent a PET/CT scan (Siemens Biograph mCT128 PET/CT, Siemens Healthcare, Erlangen, Germany) at the time of diagnosis, according to published joint procedural recommendations [11]. Patients fasted for at least 6 hours before tracer injection. Scans started 1 hour after intravenous injection of  $^{18}\text{F}$ -FDG 5 MBq per kg bodyweight. First, a native CT scan of the head was performed for attenuation correction and anatomical correlation in a supine position with arms beside the body. Acquisition parameters were 120 kV and automatic exposure with 70 mAs reference setting, pitch 0.55, slice thickness 3 mm. Next, a PET emission scan was obtained in 3D mode in one bed position, 10 minutes. Then, a native CT scan from the skull base to thighs, arms beside the head was performed (whole body scan, 120 keV, 50 mAs reference setting, pitch 0.8, slice thickness 4 mm) with a subsequent whole-body PET scan, acquisition time 90 sec per bed position. Iterative time of flight reconstruction was performed with 5 iterations and 21 subsets (skull: 2 mm FWHM Gauss filter,  $400 \times 400$  matrix; whole body: 5 mm FWHM Gauss filter,  $200 \times 200$  matrix). All PET scans were read by an experienced nuclear medicine specialist (CR; 19 years PET and PET/CT reading experience),

blinded for the diagnosis of the patients. For image analysis, SyngoVia version VB30 (Siemens Healthcare, Erlangen, Germany) was used. The trunk, frontal and parietal branches of the temporal arteries, as well as the maxillary arteries, were rated separately for both sides. Occipital arteries showed no visual uptake. Maximum SUV (SUV<sub>max</sub>) was measured individually for each vessel segment in the region with the highest visual uptake. The ratio of the SUV<sub>max</sub> of each temporal artery segment was divided by the mean liver SUV in order to calculate the SUV ratio. As described before, the temporal arteries was rated vasculitic at a SUV ratio  $>1$  [2].

### Ultrasound of the temporal artery

An iU22 or Epiq 7 ultrasound device (Philips, Best, The Netherlands) with a 17-5 MHz or 18-5 MHz transducer was used for all temporal artery ultrasound examinations. The trunk, the frontal and the parietal branches of the temporal artery on both sides were scanned in longitudinal and cross-sectional view in B-mode, as well as using the ultrasound compression sign as described before [12]. The ultrasound findings in each segment were categorised and analysed as "normal", or "vasculitis" as previously described [13]. In addition, vessel diameters of all categorised temporal artery segments were retrospectively measured. Ultrasound was performed by experienced experts (SI, MA, DS) blinded to the clinical diagnosis and the results of PET/CT.

### Histological analysis of temporal artery biopsies

Temporal artery biopsies was categorised and analysed for the following characteristics: (i) percentage of circumference of the arterial wall affected by vasculitis, (ii) amount of inflammatory infiltrate, (iii) presence of lymphohistiocytic infiltrate, (iv) presence of granulocytic infiltrate, (v) presence of giant cells, (vi) degree of intimal fibrosis and (vii) distribution pattern of the inflammation. The inflammatory infiltrate was semi-quantitatively classified as isolated inflammatory cells (+), groups of inflammatory cells separated by non-inflammatory cells (++) and confluent inflammatory cells (+++). The categorisation and analysis were made by an expert (KG) blinded to diagnosis and imaging results.

### Statistics

Continuous variables were analysed using the Mann-Whitney U-test and are expressed as medians and interquartile ranges (IQRs). Categorical variables were analysed with the chi-square or Fisher's exact test as appropriate. Correlations between quantitative values were performed using Spearman's rank order test. Statistical analysis was performed using GraphPad Prism8 (Version 8.3.0).

## Results

### Patient characteristics

Between August 2015 and January 2019, a total of 34 patients underwent PET/CT using the temporal artery protocol, 17 of whom (50%) were ultimately diagnosed with GCA. The remaining 17 patients (50%) served as controls. Controls had a final diagnoses of polymyalgia rheumatica (n = 5), arteriosclerotic anterior ischaemic optic neuropathy (n = 3), inflammatory syndromes (n = 3), papilloedema

(n = 1), granulomatous aortitis (n = 1), infection (n = 1), cholangiocellular carcinoma (n = 1), pulmonary embolism (n = 1), and diverticulitis of the sigmoid colon (n = 1). Thirteen out of the 17 GCA patients fulfilled three or more of the ACR criteria for GCA. Four fulfilled two of five ACR criteria and had either histologically confirmed vasculitis (n = 1), unequivocal vasculitis on the temporal artery ultrasound (n = 2) or large vessel vasculitis on ultrasound (n = 1) (fig. 1)

GCA patients were older than controls, but did not differ with respect to gender or systemic inflammation markers (table 1). Eight GCA patients and eight controls were corticosteroid-naïve at the time of PET/CT. One GCA patient received long-term corticosteroid therapy (5 mg) for a previous polymyalgia rheumatic diagnosis. Temporal artery

biopsy was performed in 11 GCA patients and 8 controls a median of 3 days after PET/CT (IQR 0–5 days). Detailed patient characteristics are given in table 1.

### PET/CT

Nine of 17 the patients with confirmed GCA exceeded the SUV ratio cut-off of >1 for the temporal artery, with a median SUV ratio of 1.37 for all vasculitic segments (IQR 1.15–1.52). In all the patients with confirmed GCA, there were positive findings in 35% of all trunks and 24% of all frontal branches, but in only 12% of all parietal branches. Eight of the GCA patients had no signs of vasculitis on temporal artery PET/CT (fig. 2). Seven of these were PET/CT-positive in extratemporal large vessels, according to es-

**Figure 1:** Diagnostic findings in GCA patients. ACR = American College of Rheumatology criteria for GCA; GCA = giant cell arteritis; LV US = large vessel ultrasound; TAB = temporal artery biopsy; TA PET/CT = temporal artery positron emission tomography-computed tomography; TA US = temporal artery ultrasound

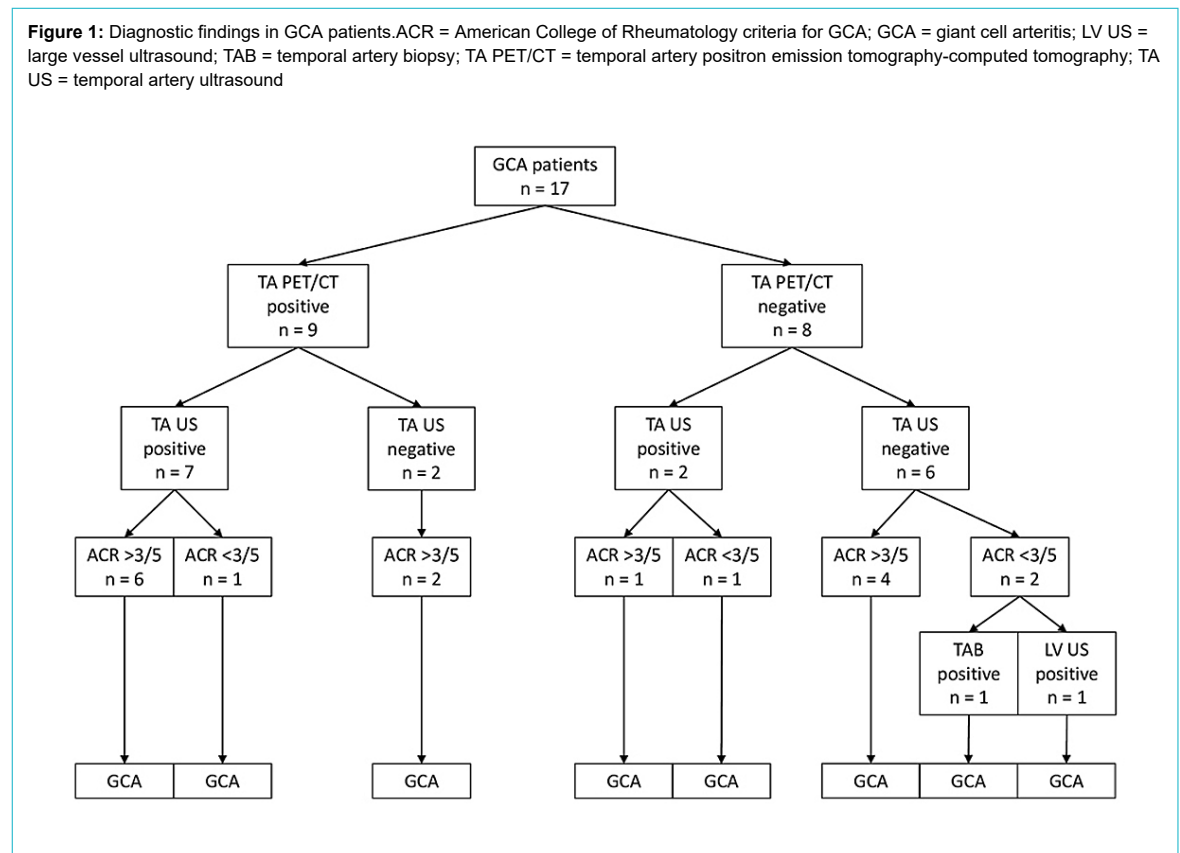


**Table 1:** Patient characteristics.

	GCA (n = 17)	Non-GCA (controls) (n = 17)	p-value
Female	10 (59)	9 (53)	>0.99
Age (years)	73 (63–78)	62 (57–72)	0.04
Amaurosis fugax / loss of vision	8 (47)	9 (53)	>0.99
New onset headache	12 (71)	11 (61)	>0.99
Jaw claudication	4 (24)	3 (18)	>0.99
Scalp tenderness / pathological temporal artery	6 (35)	6 (35)	>0.99
ESR (mm/h)	80 (54–90)	50 (27–66)	0.02
C-reactive protein (mg/l)	67 (31–130)	38 (13–129)	0.19
Glucose (mmol/l)	5.5 (5–6.2)	5 (4.7–5.5)	0.13
Cumulative glucocorticoid dose (mg) before PET/CT	350 (190–870) (n = 8)	760 (330–1810) (n = 9)	0.27
Days on glucocorticoids before PET/CT	4.5 (3.5–7) (n = 8)	4 (3–7.5) (n = 9)	0.89

ESR = erythrocyte sedimentation rate; GCA = giant cell arteritis; PET/CT = positron emission tomography-computed tomography Data are expressed as number (%) or median (interquartile range).

established criteria [2]. One patient with the final diagnosis of GCA was PET/CT-negative in both the temporal arteries and extratemporal large vessels. Positive findings in the maxillary artery occurred in three patients only. In occipital arteries, no pathological uptake was seen. Diagnostic sensitivity of PET/CT for the final diagnosis of GCA when scoring exclusively the findings within the temporal arteries was 53%, specificity was 100%. Scoring all vessels analysed in the whole-body PET/CT, but excluding the temporal arteries, resulted in a sensitivity and specificity of 88% and 59%, respectively. Combining the analysis of temporal and extratemporal arteries revealed a further increase of sensitivity to 94% and an unchanged specificity of 59%.

**Comparison of visual- and SUV ratio-based scoring of the temporal arteries**

Qualitative assessment of the branches of the temporal arteries (visible or not) alone did not result in a change of diagnostic accuracy, compared with the SUV ratio-based scoring. Sensitivity and specificity remained 53% and 100%, respectively.

**Ultrasound of the temporal arteries**

Temporal artery ultrasound was conducted a median of 2 days before PET/CT imaging (IQR 1–4.5 days). Three out of the 17 GCA patients had the ultrasound examination a median of 4 days thereafter (IQR 3–4 days).

In 9/17 GCA patients, temporal artery ultrasound showed signs of vasculitis (pathological compression sign) with homogenous distribution amongst the segments. All patients had multiple segments affected (fig. 2). For one control patient, who had an autoinflammatory syndrome, there were vasculitic ultrasound findings in the temporal arteries. Sensitivity of temporal artery ultrasound for final diagnosis of GCA was 53% and specificity was 94%.

**Comparison of PET/CT and ultrasound in individual patients and temporal artery segments**

Agreement between temporal artery PET/CT and ultrasound findings on a patient level was moderate, with seven GCA patients positive in both modalities (see fig. 3), two

on ultrasound only (see fig. 4) and two on PET/CT only. However, the distribution of vasculitic findings in individual temporal artery segments showed larger disparities, with 19 segments positive in both imaging methods, 25 on ultrasound only and 5 in PET/CT only. Pathological findings in the parietal branch of the temporal arteries could only be identified in a smaller proportion of PET/CT examinations, compared with positive findings in ultrasound or histology (fig. 2).

**Influence of the vessel diameter on <sup>18</sup>F-FDG uptake in the temporal artery branches**

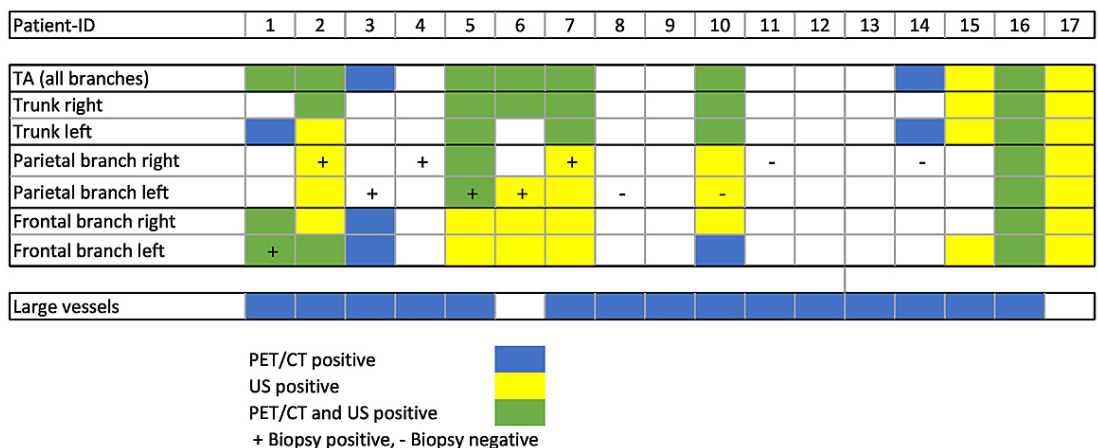
The median diameter of all trunks was 2.1 mm (IQR 1.8–2.8). Parietal and frontal branches did not differ in diameter, as measured in ultrasound (1.5 mm, IQR 1.2–1.8 vs 1.5 mm, IQR 1.1–1.7). Positive findings in PET/CT were only found in segments ≥1.4 mm, whereas the ultrasound compression sign was visible in smaller vessels down to 1.2 mm.

**Histology**

Temporal artery biopsy histology was available for 11 GCA patients and 8 controls. Biopsies in GCA patients were taken a median of 4 days after PET/CT (IQR 2–6 days) and 7 days (IQR 4–10 days) after initiation of the corticosteroid therapy. Seven of 11 biopsies from GCA patients revealed vasculitic findings. In only two of seven patients were the branches with histologically proven vasculitis also positive in PET/CT, but five of seven showed vasculitis in ultrasound at the same branch. Four patients with a positive temporal artery biopsy showed positive PET/CT findings in one of the other temporal artery branches. However, in one patient PET/CT showed no pathologies in all branches of the temporal artery despite positive biopsy findings (fig. 2).

Neither degree of histologically afflicted wall circumference, distribution of afflicted wall layers nor the number of inflammatory infiltrates revealed significant differences between PET/CT-positive and -negative patients. The degree of fibrosis was numerically higher in five PET/CT-negative GCA patients, compared with two patients with increased <sup>18</sup>F-FDG uptake in the subsequently biopsied

**Figure 2:** Distribution of positive findings in individual temporal artery (TA) segments for positron emission tomography-computed tomography (PET/CT), ultrasound (US) and temporal artery biopsy in giant cell arteritis.



branch. Patient 1 showed a low degree of fibrosis and positive findings for GCA in all diagnostic methods (fig. 3). Patient 7 revealed a higher degree of fibrosis and positive findings for GCA only in ultrasound and histology but not in the PET/CT (fig. 4).

## Discussion

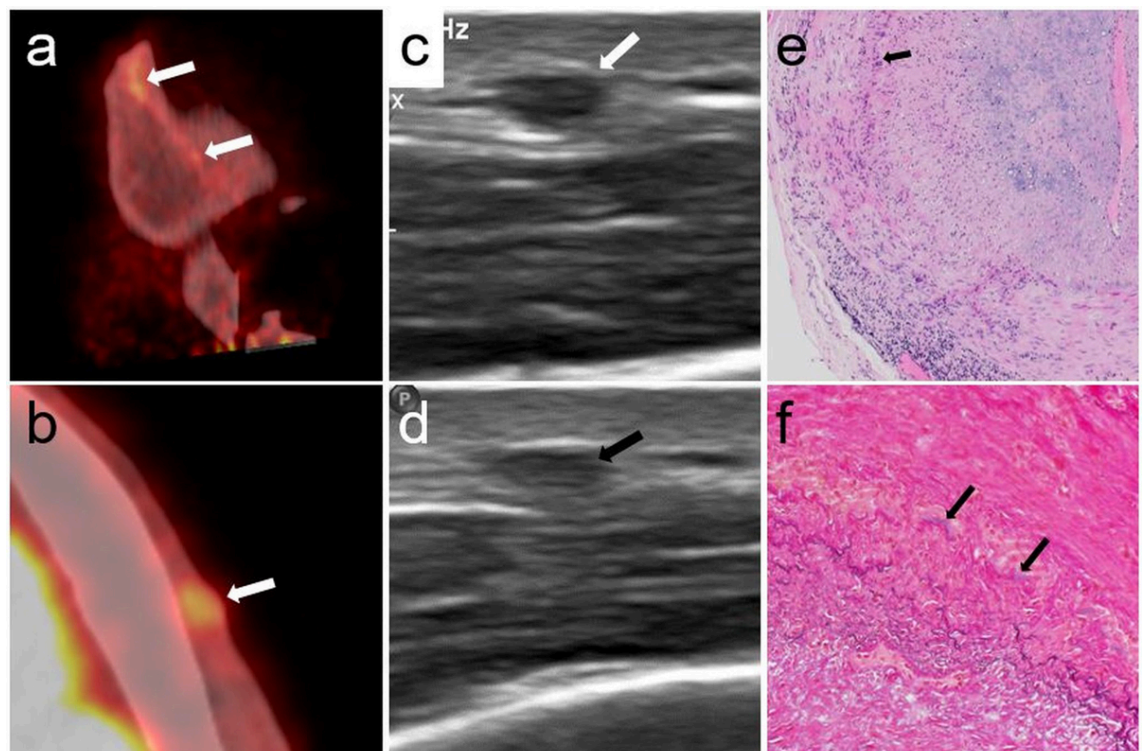
A swift and complete imaging technique, able to complement clinical and laboratory results and to confirm GCA is not established yet. Different techniques, each covering only a part of the potentially affected vessel spectrum, are well-established [14]. Modern PET/CT scanners and adjusted acquisition protocols proved to be able to visualise  $^{18}\text{F}$ -FDG uptake in the vessel wall of the temporal artery, making PET/CT a potential candidate for such a comprehensive examination. In this study, PET/CT of the temporal arteries resulted in a moderate sensitivity of 53% and excellent specificity of 100% for diagnosing GCA. Compared with the solely visual assessment, the use of a SUV ratio cut-off of 1 did not change diagnostic accuracy. Our results are comparable to those of recent studies [5, 6, 8], but show a slightly lower sensitivity when the temporal arteries only were scored. However, additional consideration of the extratemporal vessels in the whole-body PET/CT increased sensitivity to 94% and is in consequence comparable to that in the above-mentioned studies. Furthermore, we also included non-steroid-naïve patients and patients lacking cranial symptoms of temporal arteritis, which might also have affected sensitivity in our study [2].

Diagnostic accuracy of PET/CT and of ultrasound confined to the temporal arteries were comparable in our cohort, with a sensitivity and specificity of temporal artery PET/CT for the final diagnosis of 53% and 100%, compared with ultrasound at 53% and 94%, respectively. Although the diagnostic accuracy of the two modalities was similar, the classification as vasculitis or not differed in 22% of patients and in 42% of individual temporal artery segments. It has already been shown that morphological (ultrasound) and metabolic (PET/CT) imaging detect different aspects of vasculitis and are not completely congruent in the larger vessels in GCA [15].

Ultrasound seemed to be more sensitive than PET/CT in detecting vasculitis in the parietal branch. This is not due to a difference in vessel size, as the frontal and parietal branches did not differ in diameter. However, branches with a diameter <1.4 mm were not detected by PET/CT in our patients in general, which might be a technical limitation on the use of PET/CT, given the high variability of temporal artery size. The low sensitivity of PET/CT within the parietal branch might be explained by the more vertical course of this vessel compared with the frontal branch, which could impede the detection of pathological findings in the axial PET/CT images.

Uptake of  $^{18}\text{F}$ -FDG in inflamed tissue depends on the cellular components and their metabolism. We thus aimed to analyse correlation of individual inflammatory components of the temporal artery wall to PET/CT results. The low sensitivity of PET/CT for detecting vasculitis in the most often biopsied parietal branch of the temporal arter-

**Figure 3:** Patient 1, PET/CT, ultrasound and temporal artery biopsy. Sagittal (a) and axial (b) PET/CT fusion with visually positive tracer uptake (arrows) and a SUV ratio of 1.7 in the frontal branch of the left temporal artery of patient 1. Ultrasound reveals an incompressible thickened vessel wall during compression (d, black arrow), compared to before compression (c, white arrow). Lymphohistiocytic infiltrates in the media and the adventitia and severe intimal fibrosis on H and E staining (e, 100 $\times$ ). Histiocytes and giant cells (arrow) are present along the fragmented, discoloured internal elastic lamina. Van Gieson elastic stain (f, 200 $\times$ ) with only small residual fragments of the internal elastic lamina (arrows). Fibrosis of the intima (lower left) and media (upper right).



ies did not allow correlation of histological features potentially associated with higher glucose consumption with the intensity of  $^{18}\text{F}$ -FDG uptake. However, in this small cohort wall fibrosis was pronounced in the PET/CT-negative biopsied vasculitic branches (fig. 4). Future studies are needed to resolve these questions. As specificity of temporal artery PET/CT is excellent and the sensitivity of PET/CT of the extratemporal arteries can be increased by combination with temporal artery analysis, the effort of implementing the temporal artery PET/CT acquisition protocol could be beneficial. Even though the sensitivity for the temporal artery is slightly lower for PET/CT than ultrasound, the TA PET/CT protocol could be especially useful in patients with exclusive cranial manifestation as the TA PET/CT acquisition does not require much effort and does not go along with any additional radiation exposure. Furthermore, in clinical routine, a PET/CT scan serves not only the detection of suspected GCA, but is also performed in patients with systemic inflammation or fever of unknown origin. In such a situation the implementation of optimized PET/CT acquisition protocols could identify vasculitis patients with exclusively temporal artery manifestations.

Limitations of this work are the relative low number of included patients, the steroid treatment already started in half of the patients at inclusion and the fact that not all patients underwent histological confirmation of the diagnosis by temporal artery biopsy. However, this reflects daily practice.

In conclusion, PET/CT of the temporal arteries has a diagnostic accuracy similar to ultrasound. The choice between PET/CT and ultrasound for analysing the temporal arteries is not exclusive, but the methods may be complementary. In the case of a negative result with one technique, but persistent suspicion of GCA, the second technique may be diagnostic in a number of patients. We consider PET/CT including the temporal artery protocol to be a reliable “one-shot” diagnostic test with the possibility of subsequent ultrasound in the case of negative findings.

The use of PET/CT in small temporal artery branches (<1.4 mm) and in the parietal branches is limited, but might gain potential with further evolution of PET/CT scanners.

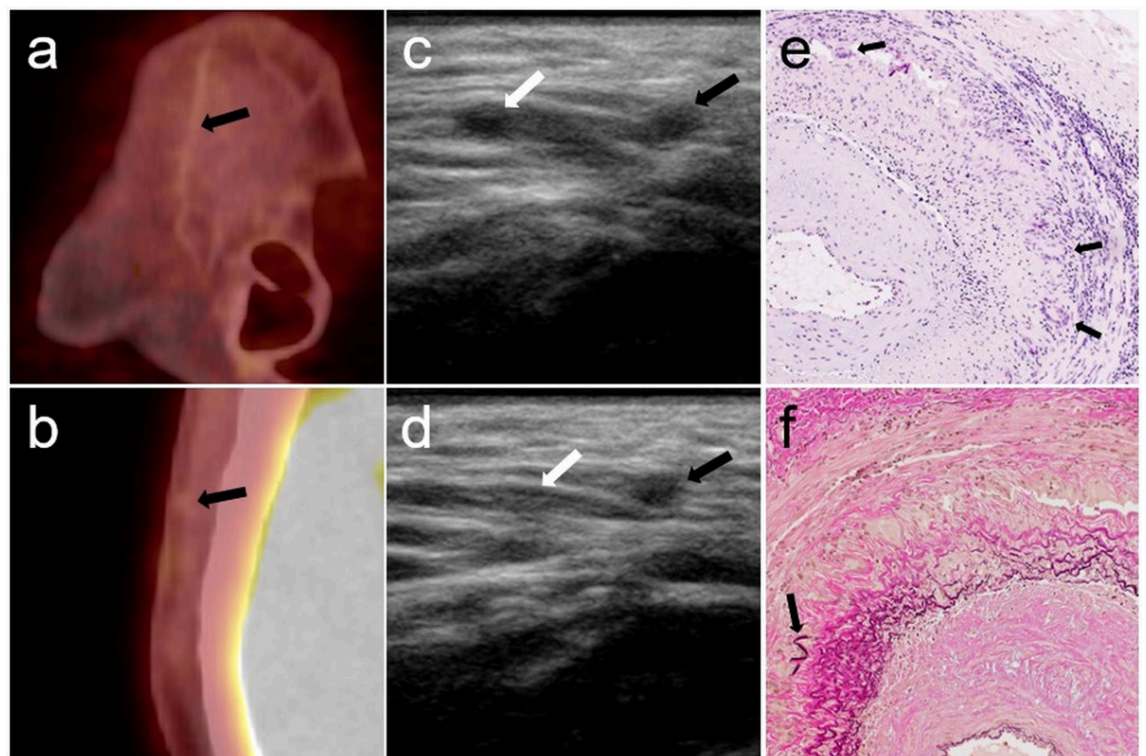
#### Disclosure statement

No financial support and no other potential conflict of interest relevant to this article was reported.

#### References

- 1 Fuchs M, Briel M, Daikeler T, Walker UA, Rasch H, Berg S, et al. The impact of  $^{18}\text{F}$ -FDG PET on the management of patients with suspected large vessel vasculitis. *Eur J Nucl Med Mol Imaging*. 2012;39(2):344–53. doi: <http://dx.doi.org/10.1007/s00259-011-1967-x>. PubMed.
- 2 Imfeld S, Rottenburger C, Schegk E, Aschwanden M, Juengling F, Staub D, et al. [ $^{18}\text{F}$ ]FDG positron emission tomography in patients presenting with suspicion of giant cell arteritis—lessons from a vasculitis clinic. *Eur Heart J Cardiovasc Imaging*. 2018;19(8):933–40. doi: <http://dx.doi.org/10.1093/ehjci/jex259>. PubMed.
- 3 Dejaco C, Ramiro S, Duftner C, Besson FL, Bley TA, Blockmans D, et al. EULAR recommendations for the use of imaging in large vessel vas-

**Figure 4:** Patient 7, PET/CT, ultrasound and temporal artery biopsy. Right parietal branch of the temporal artery of patient 7. Sagittal (a) and axial (b) PET/CT image fusion without suspected tracer uptake (arrows) and a negative SUV ratio of 0.7. Ultrasound (c and d) shows a positive compression sign in the parietal (right, black arrows), and negative sign in the frontal branch (left, white arrows) before (c) and during compression (d). The parietal branch (right) remains incompressible. A segment of the artery (e) shows dense lymphohistiocytic infiltrates in the media and the adventitia and numerous large multinucleated giant cells (arrows) along the internal elastic lamina. Heavy concentric fibrosis of the intima. (H and E, 100 $\times$ ). On van Gieson elastic stain (200 $\times$ , f) numerous giant cells are visible along the fragmented and discoloured internal elastic lamina. Fibrosis of the intima (lower right) with only small preserved fragments of the original lamina elastica interna (arrow). Several new layers of thin elastic fibres have formed in the fibrosed intima.



- culitis in clinical practice. *Ann Rheum Dis*. 2018;77(5):636–43. doi: <http://dx.doi.org/10.1136/annrheumdis-2017-212649>. PubMed.
- 4 Slomka PJ, Pan T, Germano G. Recent Advances and Future Progress in PET Instrumentation. *Semin Nucl Med*. 2016;46(1):5–19. doi: <http://dx.doi.org/10.1053/j.semnucmed.2015.09.006>. PubMed.
  - 5 Nielsen BD, Hansen IT, Kramer S, Haraldsen A, Hjorthaug K, Bogsrud TV, et al. Simple dichotomous assessment of cranial artery inflammation by conventional 18F-FDG PET/CT shows high accuracy for the diagnosis of giant cell arteritis: a case-control study. *Eur J Nucl Med Mol Imaging*. 2019;46(1):184–93. doi: <http://dx.doi.org/10.1007/s00259-018-4106-0>. PubMed.
  - 6 Sammel AM, Hsiao E, Schembri G, Nguyen K, Brewer J, Schrieber L, et al. Diagnostic Accuracy of Positron Emission Tomography/Computed Tomography of the Head, Neck, and Chest for Giant Cell Arteritis: A Prospective, Double-Blind, Cross-Sectional Study. *Arthritis Rheumatol*. 2019;71(8):1319–28. doi: <http://dx.doi.org/10.1002/art.40864>. PubMed.
  - 7 Hunder GG, Bloch DA, Michel BA, Stevens MB, Arend WP, Calabrese LH, et al. The American College of Rheumatology 1990 criteria for the classification of giant cell arteritis. *Arthritis Rheum*. 1990;33(8):1122–8. doi: <http://dx.doi.org/10.1002/art.1780330810>. PubMed.
  - 8 Nienhuis PH, Sandovici M, Glaudemans AW, Slart RH, Brouwer E. Visual and semiquantitative assessment of cranial artery inflammation with FDG-PET/CT in giant cell arteritis. *Semin Arthritis Rheum*. 2020;50(4):616–23. doi: <http://dx.doi.org/10.1016/j.semarthrit.2020.04.002>. PubMed.
  - 9 Unizony SH, Dasgupta B, Fischeleva E, Rowell L, Schett G, Spiera R, et al. Design of the tocilizumab in giant cell arteritis trial. *Int J Rheumatol*. 2013;2013:912562. doi: <http://dx.doi.org/10.1155/2013/912562>. PubMed.
  - 10 Bardi M, Diamantopoulos AP. EULAR recommendations for the use of imaging in large vessel vasculitis in clinical practice summary. *Radiol Med (Torino)*. 2019;124(10):965–72. doi: <http://dx.doi.org/10.1007/s11547-019-01058-0>. PubMed.
  - 11 Slart RHJA; Writing group; Reviewer group; Members of EANM Cardiovascular; Members of EANM Infection & Inflammation; Members of Committees, SNMMI Cardiovascular; Members of Council, PET Interest Group; Members of ASNC; EANM Committee Coordinator. FDG-PET/CT(A) imaging in large vessel vasculitis and polymyalgia rheumatica: joint procedural recommendation of the EANM, SNMMI, and the PET Interest Group (PIG), and endorsed by the ASNC. *Eur J Nucl Med Mol Imaging*. 2018;45(7):1250–69. doi: <http://dx.doi.org/10.1007/s00259-018-3973-8>. PubMed.
  - 12 Aschwanden M, Daikeler T, Kesten F, Baldi T, Benz D, Tyndall A, et al. Temporal artery compression sign--a novel ultrasound finding for the diagnosis of giant cell arteritis. *Ultraschall Med*. 2013;34(1):47–50. doi: <http://dx.doi.org/10.1055/s-0032-1312821>. PubMed.
  - 13 Aschwanden M, Kesten F, Stern M, Thalhammer C, Walker UA, Tyndall A, et al. Vascular involvement in patients with giant cell arteritis determined by duplex sonography of 2x11 arterial regions. *Ann Rheum Dis*. 2010;69(7):1356–9. doi: <http://dx.doi.org/10.1136/ard.2009.122135>. PubMed.
  - 14 Berger CT, Sommer G, Aschwanden M, Staub D, Rottenburger C, Daikeler T. The clinical benefit of imaging in the diagnosis and treatment of giant cell arteritis. *Swiss Med Wkly*. 2018;148:w14661. doi: <http://dx.doi.org/10.4414/smw.2018.14661>. PubMed.
  - 15 Imfeld S, Aschwanden M, Rottenburger C, Schegg E, Berger CT, Staub D, et al. [18F]FDG positron emission tomography and ultrasound in the diagnosis of giant cell arteritis: congruent or complementary imaging methods? *Rheumatology (Oxford)*. 2020;59(4):772–8. doi: <http://dx.doi.org/10.1093/rheumatology/kez362>. PubMed.